

1 **Dominant Effect Of Host Genetics On Skin Microbiota Composition In Homeostasis And**  
2 **Wound Healing**

3 Jack Galbraith<sup>1</sup>, Julien M. D. Legrand<sup>1,2</sup>, Nicholas Muller<sup>1,3</sup>, Betoul Baz<sup>1,4</sup>, Katie Togher<sup>3</sup>,  
4 Nicholas Matigian<sup>5</sup>, Seungha Kang<sup>3</sup>, Sylvia Young<sup>7</sup>, Sally Mortlock<sup>6</sup>, Edwige Roy<sup>1</sup>, Grant  
5 Morahan<sup>7</sup>, Graeme Walker<sup>1\*</sup>, Mark Morrison<sup>3\*</sup>, Kiarash Khosrotehrani<sup>1\*</sup>

6

7

8 1. The University of Queensland, UQ Diamantina Institute, Experimental Dermatology Group,  
9 Brisbane, Australia

10 2. Australian Regenerative Medicine Institute, Monash University, Clayton, Victoria,  
11 Australia.

12 3. The University of Queensland, UQ Diamantina Institute, Microbial biology and  
13 metagenomics group, Brisbane, Australia

14 4. National Centre for Genomic Technologies, King Abdul Aziz City for Science and  
15 Technology, Riyadh, Saudi Arabia

16 5. QCIF Facility for Advanced Bioinformatics, Institute for Molecular Bioscience, The  
17 University of Queensland, St Lucia, Brisbane, QLD Australia

18 6. Institute for Molecular Bioscience, The University of Queensland, St Lucia, Brisbane, QLD  
19 Australia

20 7. Centre for Diabetes Research, The Harry Perkins Institute for Medical Research, University  
21 of Western Australia, Perth, WA, Australia

22

23 \*Contributed equally as senior authors

24

25 Corresponding author:

26 Kiarash Khosrotehrani, MD PhD FACD

27 The University of Queensland Diamantina Institute

28 Translational Research Institute  
29 37 Kent Street, Woolloongabba 4102 QLD, Australia  
30 Email: [k.khosrotehrani@uq.edu.au](mailto:k.khosrotehrani@uq.edu.au)  
31

## 32 **Abstract**

33           Animal microbiota are shaped and maintained not only through microbiota-  
34 environmental interactions but also through host-microbiota interactions. The effects of the  
35 microbiota on the host has been the source of intense research in recent years, indicating a role  
36 for resident microbes in a range of conditions from obesity and mood disorders to atopic  
37 dermatitis and chronic wounds. Yet the ability of hosts to determine their microbiota  
38 composition is less well studied. In this study, we investigated the role host genetics plays in  
39 determining skin microbiota. We used 30 different mouse strains from the advanced  
40 recombinant inbred mouse panel, the Collaborative Cross, with PERMANOVA, GWAS and  
41 PCA-based GWAS analyses to demonstrate that murine skin microbiota composition is  
42 strongly dependent on murine strain. In particular, a quantitative trait locus on chromosome 4  
43 associates both with *Staphylococcus* abundance and principal-component multi-trait analyses.  
44 Additionally, we used a full thickness excisional wound healing model to investigate the  
45 relative contributions from the skin microbiota and/or host genetics on wound healing speed.  
46 Wound associated changes in skin microbiota composition were observed and were in many  
47 instances host-specific. Despite reaching statistical significance, the wound-associated changes  
48 in skin microbiota accounted for only a small amount of the variance in wound healing speeds,  
49 with the majority attributable to mouse genotype (strain) and age. Host genetics has a  
50 significant impact on the skin microbiota composition during both homeostasis and wound  
51 healing. These findings have long reaching implications in our understanding of associations  
52 between microbiota dysbiosis and disease.

## 53 **Introduction**

54 All animals are colonised by microbes soon after birth. In recent years, these  
55 “microbiomes” have been implicated in a wide range of host responses relevant to homeostasis,  
56 and their disruption can manifest in a wide range of immune-mediated and/or metabolic-related  
57 diseases [1, 2]. The gut (stool) microbiome has been the most intensively studied and has  
58 advanced the concept of “community-based” interactions, that trigger a range of conditions  
59 such as atopic dermatitis, obesity or mood disorders [3-5]. Although less studied, variations in  
60 the skin microbiome have been associated with episodes of atopic dermatitis [6], and the  
61 healing rate of leg ulcers, among other conditions [7, 8]. The skin microbiome has been shown  
62 to vary with anatomical location and patient age [9], and environmental cues such as humidity  
63 and/or temperature may also influence inter-individual variation [10]. In that context, diet is  
64 now also considered to exert a strong effect on the microbiome that can in turn influence host  
65 response and health status [2]. Overall, many environmental factors seem to determine the  
66 composition of the skin microbiota.

67 However, there are relatively few studies that provide a systematic assessment of how  
68 host genotype affects microbiome composition. Broader genome-wide studies utilising inter-  
69 cross mouse panel (BXD) have identified many host-specific quantitative trait loci (QTL)  
70 affecting gut microbiome composition, with candidate genes involving cytokines and toll-like  
71 receptor signalling [11]. In addition, investigation of the gut microbiota of mice from another  
72 advanced inter-cross model found 18 separate QTL associated with the relative abundance of  
73 one or more gut bacterial taxonomies [12]. Regarding skin, most studies to date have been  
74 limited to candidate approaches, such as how mutations affecting the serine protease matriptase  
75 can lead to a shift in the skin microbiota composition [13], or have described the skin microbial  
76 populations more generally [14-16]. In addition, many studies investigating wounds and skin  
77 microbiome associations have focused on non-healing chronic wounds such as diabetic foot  
78 ulcers and venous leg ulcers [17-19]. Whether host genetics also affects the wound  
79 microbiome, or alternatively, whether the environmental changes associated with wounding  
80 dominate over the effect of host genetic and more strongly affect microbial composition, are  
81 unknown.

82 Here we utilised a resource generated by a specialised breeding program, the  
83 Collaborative Cross (CC), which through a recombinant-inbreeding design, allows  
84 interrogation of complex traits and genetic pleiotropies [20, 21]. Using 30 different CC mouse

85 strains, we investigated the host genetic contribution to mouse dorsal skin microbiota  
86 composition during homeostasis and wound healing. We found that the cutaneous microbiota  
87 composition differed between mouse strains, and that responses to wounding related to their  
88 microbiome composition were strain-specific. Genome-wide association studies (GWAS)  
89 identified key QTL associated with specific bacterial taxa from normal skin. Host genetics not  
90 only accounts for most of the observed variation in microbiome composition of normal skin,  
91 but also affects wound healing speed, while microbiota composition was found to only have a  
92 limited role in the latter process.

93

## 94 **Results**

### 95 *Murine strain is a strong determinant of microbiota diversity*

96 The diversity of the skin microbiome has been shown to vary between individuals and  
97 can often associate with pathological states. Here we collected swabs of mouse dorsal skin for  
98 16S rRNA gene amplicon sequencing to investigate differences in microbiome composition  
99 between mouse strains. For each mouse, swabs were collected in a predefined area of the dorsal  
100 skin in a reproducible way. Control swabs (sham swabbing), swabs taken of skin immediately  
101 after full-excisional wounding, for each mouse, did not result in any significant amplification  
102 of 16S rRNA gene. We first compared the Shannon's diversity metric as a measure of alpha-  
103 diversity (within sample) across 114 mice from 30 different mouse strains using the R package  
104 'vegan'. The microbiota profiles from most mice fell within a relatively narrow range of  
105 Shannon's diversity values (IQR=0.59, median=2.11), but communities in some mice clearly  
106 displayed less diversity and/or evenness (**Fig. 1a**). Additionally, the intra-strain variation in  
107 Shannon's diversity values was generally small, but the inter-strain variation, as measured by  
108 Kruskal-Wallis testing was large and significant ( $p<0.0001$ ). Importantly, the clustering of  
109 mice within their respective strains was also established, more generally, with their skin  
110 microbial composition (family level) by Ward's method of agglomerative hierarchical  
111 clustering [22, 23] (**Fig. 1b**). This analysis revealed that the large heterogeneity in overall  
112 mouse skin microbiota composition was strongly strain-dependent, which was further  
113 confirmed by PERMANOVA (R-squared > 0.5,  $p=0.001$ ). We next asked whether specific  
114 microbial genera were associated specifically with lower or higher diversity compositions  
115 ('ALDEx2' R package). The abundances of both *Staphylococcus* and *Aerococcus* spp.  
116 significantly differed across the highest and lowest quartiles of Shannon's diversity values,

117 respectively (*Staphylococcus*  $p=0.0019$ , *Aerococcus*  $p=0.0028$ ). A linear regression model  
118 using Shannon's diversity and the centred-log ratio (CLR) transformation of the abundance  
119 values for *Staphylococcus* and *Aerococcus* across all mice showed there was an inverse  
120 relationship of both genera with the Shannon's diversity value of mouse skin microbiome  
121 (**Supp. 2c**).

122

### 123 *Skin microbiota composition is determined by murine strain specific genomic loci.*

124 Next, we determined a core skin microbiome and used different levels of bacterial  
125 taxonomies to identify their representation in at least 50% of samples at 0.1% or greater relative  
126 abundance. Similar to the broader composition, core microbiome of individual mice clustered  
127 within their respective strains (Ward's method of agglomerative hierarchical clustering) and  
128 significant groupings at the family-level of classification were found and could be further used  
129 to categorise the different host genotypes (**Fig. 1b**). While *Staphylococcaceae* was the most  
130 prevalent bacterial family in the strains of mice examined, and thereby a member of the core  
131 microbiome, there was also a group of mouse strains that clustered based on their possession  
132 of a relatively high abundance of *Corynebacteriaceae* (**Fig. 1b & Fig. 1c**). Although mouse  
133 age significantly affected skin microbiome profile, it was found to explain only a minimal  
134 amount of the variance observed across mice (R-squared < 0.02). Taken together, these  
135 findings strongly confirmed the effect of murine strain (host genotype) as a key determinant of  
136 the dorsal skin microbiome.

137 Given these findings, we next examined whether specific loci in the mouse genome  
138 could be associated with the dorsal skin microbiome composition. The centred log-ratio  
139 transformation of the abundance values for *Staphylococcus* was used as a "trait" for host  
140 genome-wide association analysis using the GeneMiner software, and identified a genome-  
141 wide significant region on mouse chromosome (Chr) 4 between 129.75-130.95 megabase pairs  
142 (Mbps) (LOD Score: 10, **Supp. 1a**). Several different loci, albeit with weaker (suggestive)  
143 LOD scores were identified using both centred-log ratio transformation of the abundance  
144 values for *Aerococcus* (Chr 13, 108.70-113.51 Mbps, LOD Score: 6, **Supp. 1b**), and Shannon's  
145 diversity scores (Chr 15, 3.20-7.40 Mbps, LOD Score: 8, **Supp. 1c**), along with principal  
146 component analysis (PCA)-based GWAS, which is an approach to identify multi-trait loci from  
147 multi-dimensional data [24] (**Supp. 1d-e**). Interestingly, the peak on Chr 4 identified for  
148 *Staphylococcus* was also recovered using the PCA-based GWAS (**Supp. 1e**). A detailed  
149 analysis of the founder haplotypes for the Chr 4 candidate region identified the WSB and PWK

150 founder alleles associated with a relatively low abundance of *Staphylococcus* in skin  
151 microbiome, and the CAST founder allele with highest relative abundances. We next examined  
152 this region of interest for any genes harbouring specific polymorphisms in the founder  
153 haplotypes above, by using the Sanger Mouse Genome Project SNP query website. Here, we  
154 identified *Ptafr* as a candidate gene of interest, on the basis that its product may affect the  
155 immune response to pathogens [25, 26], but is also known to act directly on the wound healing  
156 process [27], and can affect skin inflammation [28]. An alternative candidate is *Smpdl3b*,  
157 *Sphingomyelin Phosphodiesterase Acid-Like 3B*, which is associated with inflammation via  
158 negative regulation of toll-like receptor signalling *in vivo* [29]. A full list of genes containing  
159 haplotype specific SNP is provided in **Suppl. 3**. Overall, this strong effect of murine strain, as  
160 well as the association with plausible candidate genes, strongly supports the importance of host  
161 genetics in determining the skin microbiome during homeostasis.

162

### 163 *The microbiomes of early stage wounded and normal skin retain host-strain specificity*

164 We next investigated whether and how wounding, considered a major environmental  
165 stress, would elicit stronger effects on the microbiome than host genotype. If skin injury and  
166 wound healing had strong effects on the microbiome, one would expect the wound microbiome  
167 to be convergent across the different mouse strains. Alternatively, given the exposure to faecal  
168 material in the cage bedding, one would expect the wound and faecal microbiome to converge.  
169 To that end, we performed PCA and hierarchical clustering on the combined datasets from  
170 unwounded skin, day (D) 3 wounds, and the faecal microbiome samples of 70 mice  
171 representing the different haplotypes. Importantly, the DNA extractions of the swab samples  
172 collected immediately after wounding did not produce sufficient 16S rRNA gene amplicons,  
173 suggesting that the debrided area was made “sterile” by the wounding process at D0. We found  
174 that the wound microbiome at D3 retained its similarity to the community present on  
175 unwounded skin, and that the faecal microbiomes were clearly separable from the skin and  
176 wound microbiomes using PCA and hierarchical clustering (**Fig. 2a-b**). The bacterial families  
177 *Propionibacteriaceae* and *Staphylococcaceae* were discriminatory for both the unwounded  
178 skin and wound microbiomes at D3, compared to faecal samples, and *Bacteroidales* family  
179 S24-7 were in much greater abundance in faecal samples (**Supp. 2a**). However, while the D3  
180 wound microbiomes still retained features of normal skin, there was a significant decline in  
181 diversity between unwounded and D3 skin wound microbiomes (**Fig. 2c**, Mann-Whitney,  $p$ -  
182 value<0.0001, 0.788 median fold-change in Shannon’s diversity across all mice). This decline

183 in diversity recapitulates that seen in other pathologies such as eczema flares, and some non-  
184 healing diabetic foot ulcers [14, 17]. The declines in microbial diversity of the wounds were  
185 only transient however, and diversity had recovered significantly by D10 post-wounding via  
186 Kruskal-Wallis testing ( $p < 0.01$ , 1.1 median fold-change in Shannon's diversity across all  
187 mice), but still remained significantly lower than the original unwounded skin at this time-point  
188 ( $p < 0.01$ , 0.8 median fold-change unwounded to D10 Shannon's diversity).

189 We also evaluated whether the 'core' microbiome differed between wounded (D3) and  
190 unwounded skin. The hierarchical clustering (**Fig. 3a**) showed that although there was a general  
191 trend of increased *Staphylococcaceae* and *Corynebacteriaceae* relative abundances between  
192 D3-wounded and unwounded skin (FDR-adjusted,  $p < 0.1$ , ALDEX2), some mouse strains  
193 showed a decrease in these families. This clearly highlighted that the changes of microbiota  
194 composition in response to wound healing were not universal and varied across murine strains.

195 To investigate the relative contributions to changes in microbiota composition during  
196 wound healing, a PERMANOVA analysis was performed with the variables being mouse  
197 strain, wound time-point (unwounded or D3) and mouse age (days). The strain of mouse had  
198 the largest effect on overall microbiome compositional changes during wound healing (~23%  
199 variance explained), followed by the interaction between mouse strain and wound time-points  
200 (~17% variance explained). While statistically significant, age and wound time-point alone  
201 accounted for only a small amount of variance (<8% combined). This once again strongly  
202 supports the effect of host genotype on both the unwounded and wounded skin microbiomes.

203

#### 204 ***Microbiome composition had minimal effect on wound healing rates***

205 Given the variation between mice in their D3 post-wounding microbial composition and the  
206 microbiota differences from unwounded skin, we investigated whether these parameters were  
207 associated with wound healing. The time to wound closure for individual mice was  
208 determined and used to group these into quartiles representing fast to slow healers. Compared  
209 to unwounded skin, there were large variations, both positively and negatively, in the relative  
210 abundances of different bacterial families present in D3 wound microbiomes assigned to the  
211 different quartiles (**Fig. 3b**). However, these changes in the skin/wound microbiomes during  
212 early wound healing, and the faecal microbiome composition of the host animal each  
213 accounted for ~5% of the variance in wound healing speeds when modelled separately by  
214 principal component regression. In contrast, PERMANOVA analysis showed mouse strain



215 (genotype) accounted for over 50% of the variance in wound healing rate ( $p < 0.001$ ) while the  
216 age of mice explained 20% variance ( $p$ -value  $< 0.001$ ). Age is already recognised to be a  
217 significant factor in the regenerative ability of mice [30, 31]. Our results not only confirm the  
218 association between mouse age and wound healing speed, but the limited impact of age on  
219 skin microbiome composition suggests the impacts of age on wound healing speed are host-  
220 rather than microbiome-related.

221

## 222 **Discussion**

223 The skin microbiome has been the subject of many studies because of its presumed  
224 involvement with the onset and/or progression of many skin disorders [5-7, 14, 17, 19, 32].  
225 Many studies have revealed how (micro) environmental factors such as temperature, humidity,  
226 dryness, sun exposure, body site, or host factors such as age and diet can affect the skin  
227 microbiome [5, 9, 10, 33]. These collective findings have led many to infer that wounding -  
228 which is an extreme form of environmental insult - results in a stereotypical change in the  
229 composition of the microbiome at the wound site, principally via increases in the relative and  
230 total abundances of *Staphylococcus* and Gram-negative bacteria [32, 34]. In contrast, very little  
231 is known about whether and how host genotype affects the skin microbiome, and further, to  
232 what extent differences in wound healing speed are attributable to host-driven processes either  
233 directly, or indirectly, via the skin microbiome.

234 By characterization of multiple strains of mice from the Collaborative Cross, we show  
235 that while the skin microbiome is strongly impacted by host genotype, there is only a small  
236 contribution from this microbiome variation to wound healing speed. Further, we showed a  
237 strong variation in skin microbiota composition that in large part was explained by the murine  
238 genetic background. Importantly, all the animals used in this study were born in the same  
239 animal facility; then all shipped and subsequently housed in a different facility and provided  
240 access to the same food and water sources. So while it is not possible to completely rule out  
241 any housing effects across all 30 strains of mice, other studies have revealed that compared to  
242 host genotype, the contributions from caging and legacy effects on the variations in the gut  
243 microbiome are small [35]. Additional studies of skin bacterial populations in various  
244 mammals and amphibians further supports host taxonomy as a greater determining factor of  
245 the cutaneous microbiome than environment [36-38].

246 In that context, the genome-wide associations identified key host loci predictive of  
247 specific skin bacterial taxa and/or microbiome composition. Indeed, specific bacterial genera  
248 (*Staphylococcus* and *Aerococcus*) and Shannon diversity scores of the skin microbiome from  
249 individual mice could be used as a “trait” in genome wide association and linkage studies. In  
250 particular, these analyses defined a ~1 Mbp region on Chr 4 to be strongly associated with these  
251 traits. Further analyses confirmed this locus includes genes affecting host innate and adaptive  
252 immunity and in particular *Ptafr*, which encodes the Platelet Activating Factor Receptor. The  
253 PTAFR protein has strong pro-inflammatory effects and has been previously associated with  
254 bacteraemia [25, 26, 28]. Similarly, *Smpdl3b*, Sphingomyelin Phosphodiesterase Acid-Like  
255 3B, is associated with inflammation via negative regulation of toll-like receptor signalling in  
256 vivo [29]. While the precise role of these candidate genes needs experimental validation, it is  
257 plausible that SNP variations in one or both of these genes can elicit differential immune or  
258 dermal niche alterations that affect the relative abundance of *Staphylococcus* and/or  
259 *Aerococcus* on skin.

260 Abundance of *Staphylococcus* and *Aerococcus* was associated with lower diversity in  
261 homeostatic skin microbiota. The *Staphylococcus* genus contains both commensal and  
262 pathogenic species, such as *staphylococcus epidermidis* and *staphylococcus aureus*. Host  
263 *NOD2* receptor variants have been associated with atopic dermatitis and can affect keratinocyte  
264 susceptibility to *S. aureus* [39]. Additionally, previous authors have shown an expansion of the  
265 *S. aureus* population is associated with pathogenic states, such as eczema flares [14]. One study  
266 in diabetic men showed a higher Staphylococcal abundance in healthy controls compared to  
267 diabetics, yet the proportion of *S. aureus* was lower in controls indicating that some less  
268 virulent Staphylococcal species are likely protective [18]. Interestingly, *S. epidermidis* can help  
269 co-ordinate the host’s response to *S. aureus* by inducing host cytokines that influence T-cell  
270 behaviour [40]. Whilst our data supports other’s findings of a host effect on Staphylococcal  
271 species abundance and skin microbiota diversity, it is unclear whether the changes we see in  
272 Staphylococcal abundance include expansions of pathogenic or commensal species, as we were  
273 unable to investigate taxonomies to the species level. An important implication of our study is  
274 that microbiome dysbiosis in disease may only be restored temporarily through intervention  
275 such as probiotics, as the genetic background of the individual may have a dominant role.

276 In a clinical setting, it has been thought that skin wounds are characterised by major  
277 colonisation of Gram-negative bacteria, such as *Pseudomonas aeruginosa* [34], and often  
278 display an over-representation of Staphylococci [32]. Here, we report that wound microbiome

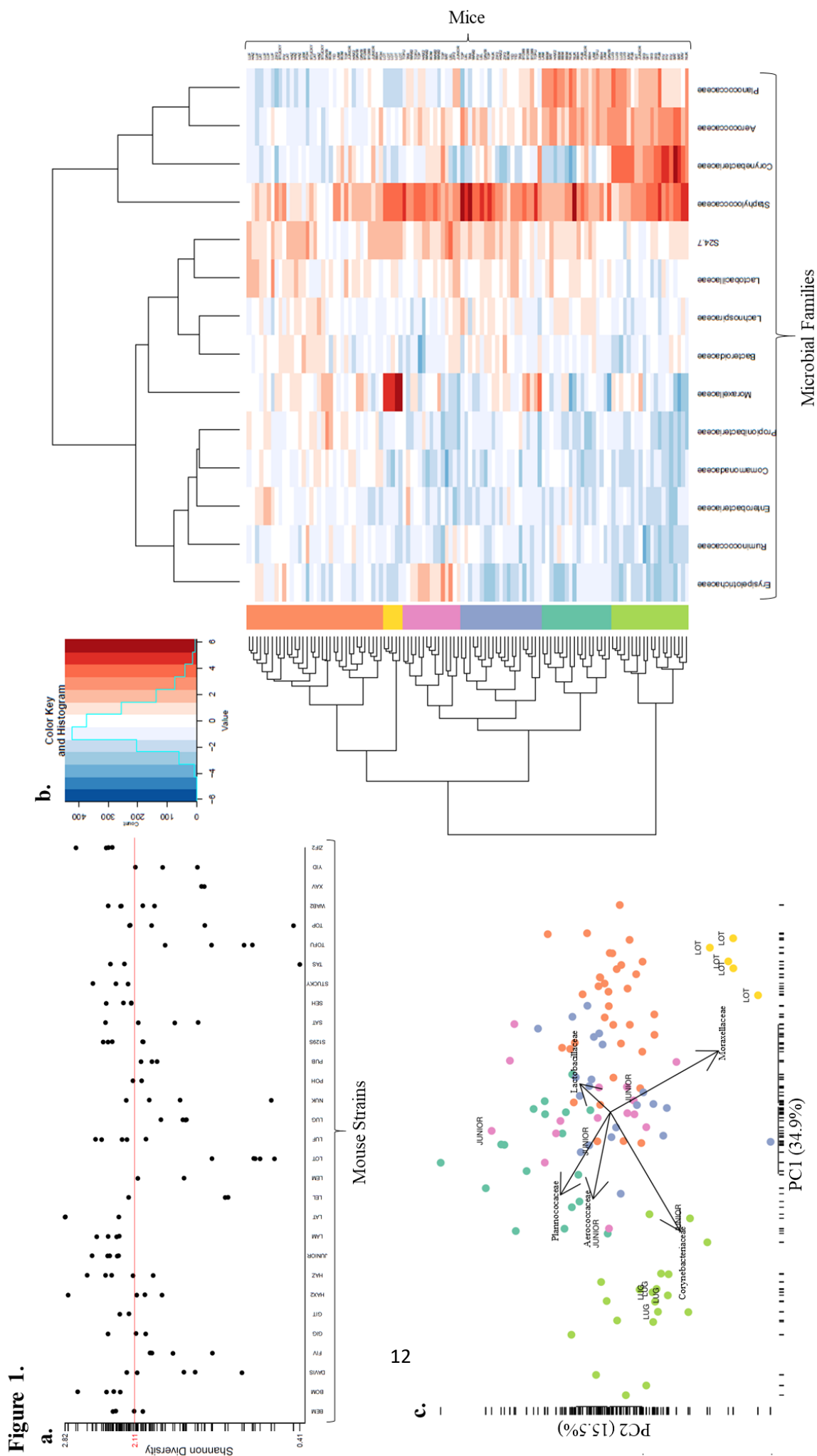
279 remains highly variable in its composition across different murine strains and there was no  
280 homogenous change across all mice. Inclusion of stool samples allowed us to show that D3  
281 post-wound skin retains a skin-like microbiota phenotype. This is unexpected given the  
282 extreme barrier function dysregulation as well as the relative contamination of cage bedding  
283 with faeces. Considering the site specificity and stability of the human microbiome [9], it is  
284 possible that the transcriptomic environment of skin wounds drives the microbiota to retain  
285 its skin-like features.

286         Few studies of murine microbiota composition of skin have utilised multiple strains of  
287 mice; a majority used only a single mouse genetic background [37, 41]. Our study highlights  
288 the difficulty of drawing conclusions about microbial associations with wound healing  
289 outcomes across studies that have used a single background mouse model of microbiota  
290 changes. Studies of chronic wounds in patients show relatively little difference in the more  
291 abundant genera between healing and non-healing wounds [42]. In line with these results, we  
292 were unable to identify any statistically significant, or suggestive, abundant microbial families  
293 associated with healing speed in mice, although we were able to show suggestive differences  
294 in microbial compositional changes between mouse strains during the early stages of wound  
295 healing. Principal component regression showed that both faecal and skin microbiomes account  
296 for minimal differences in wound healing speed. Additionally, PERMANOVA analysis shows  
297 that the strain of mouse, and its interaction with the wound time-course, can explain ~40% of  
298 variance in microbiota composition changes during the first 3 days of wound healing. Whilst  
299 lack of significant associations between microbiota abundances and wound healing speeds  
300 could be due to omission of low abundance microbes, significant heterogeneity in microbiota  
301 composition between mouse strains, and their specific response to wounding, likely plays a  
302 dominating role.

303         In conclusion, we report that skin murine microbiota and its changes upon wounding  
304 are strongly determined by host genetics and the abundance of specific microbial families can  
305 be determined by precise loci in the murine genome. Moreover, the wound microbiome plays  
306 a minimal role in the healing rate and is mostly a reflection of the host genetic background.  
307 These findings have far reaching implications for the design of further studies on the role of  
308 the microbiome on health and disease as well as the use of probiotics in a clinical setting.

309

310

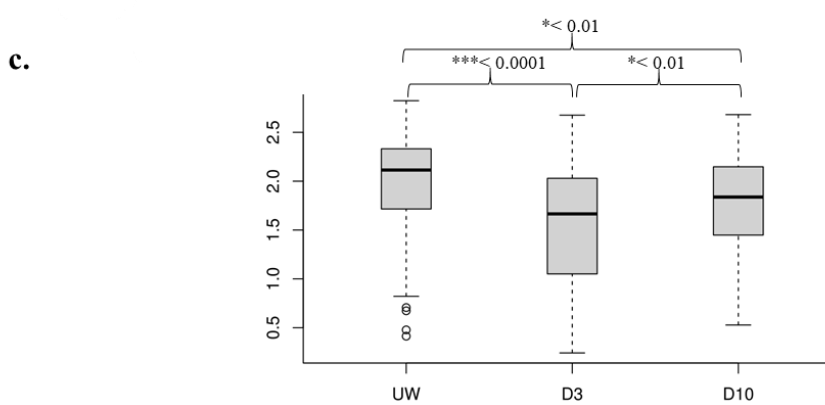
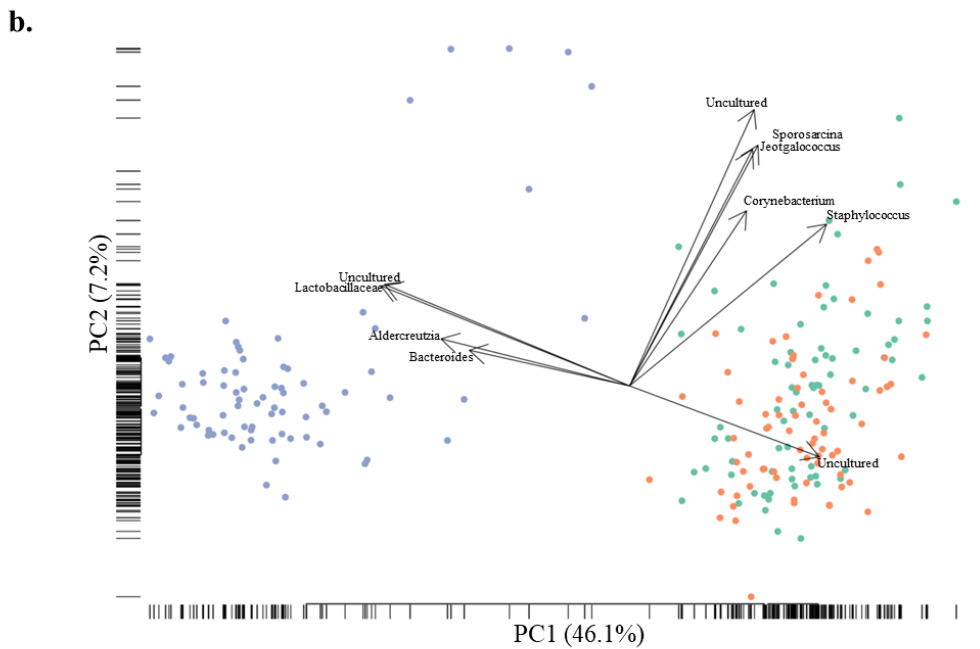
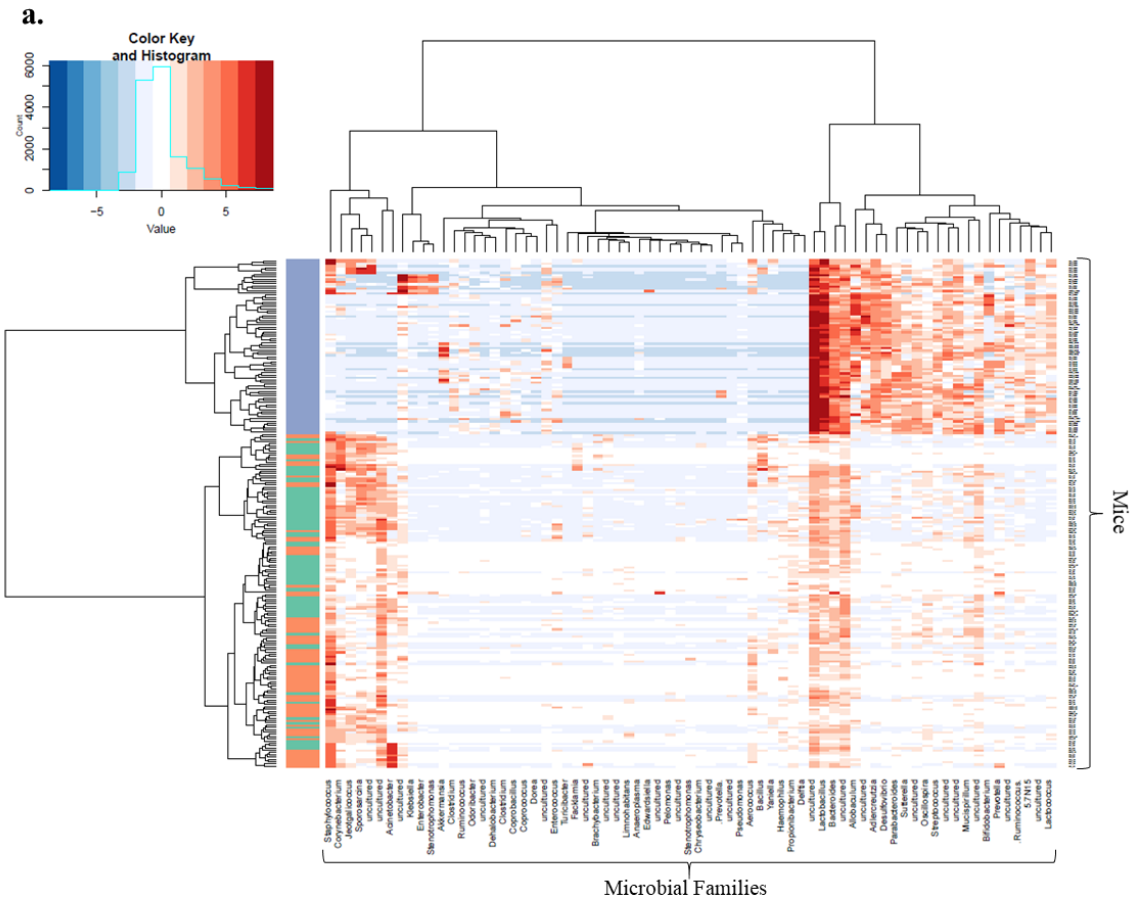


312 **Figure 1. An overview of the cutaneous microbiota across 30 different strains of mice**  
313 **from the Collaborative Cross. (a)** Scatterplot of alpha diversities for each sample, grouped  
314 by mouse strain. Most mice show similar alpha-diversities (Shannon, IQR=0.59, median=2.11)  
315 with many strains showing low intra-strain variability. Some strains such as TOFU and LUG  
316 show lower diversity scores in all mice within their strain, additionally some strains show much  
317 larger intra-strain variabilities, such as TAS and TOP. Diversity of the skin microbiome shows  
318 strong strain dependent differences (Kruskal-wallis,  $p$ -value<0.0001). **(b)** Hierarchical  
319 clustering heat-map of `core` microbiota, centred-log ratio read counts of 16S rRNA gene  
320 sequencing of healthy dorsal skin swabs. *Staphylococcaceae* was the most abundant bacterial  
321 family in the majority of mice, with *Corynebacteriaceae* showing a particularly partisan  
322 abundance across different mice. Many mice cluster strongly within their respective strain, with  
323 PERMANOVA analysis indicating a significant strain effect (R-squared>0.5,  $p$ -value=0.001).  
324 We cut the hierarchical dendrogram into 6 groups (colours randomly assigned to each group)  
325 based on visual inspection resulting in distinct characteristics such as high *Corynebacteriaceae*  
326 or *Moraxellaceae* abundance. **(c)** Principal component analysis of centred-log ratio read counts  
327 further highlights the differences in abundance of microbiota families between mice. Some  
328 strains such as LUG and LOT can be seen clustering very closely together indicating a strong  
329 strain effect. With that said, the strain JUNIOR shows that not all mouse strains have a strong  
330 preference toward certain microbiota compositions.

331

332

**Figure 2.**



333 **Figure 2. Comparison of diversity and composition of faecal, unwounded and wounded**  
334 **skin microbiota (a)** Hierarchical clustering heatmap of centred-log ratio read counts from all  
335 3 sample microbiota types (faecal = blue, unwounded = green, day-3 post-wounding = orange).  
336 Both types of skin microbiota samples show enrichment in certain bacterial genera such as  
337 *Staphylococcus*, *Corynebacterium* and *Acinetobacter* compared to faecal samples. **(b)**  
338 Principal component analysis of combined sample sets at the genus level. Day-3 post-wound  
339 microbiota cluster with unwounded microbiota samples and separately from faecal samples  
340 (faecal = blue, unwounded = green, day-3 post-wounding = orange). **(c)** Skin microbial  
341 diversity at different time-points (Shannon alpha diversity index). Overall alpha diversity  
342 significantly decreases from unwounded to day-3, increasing again by day-10 though  
343 remaining significantly depressed compared to unwounded skin.

344

345

346

347

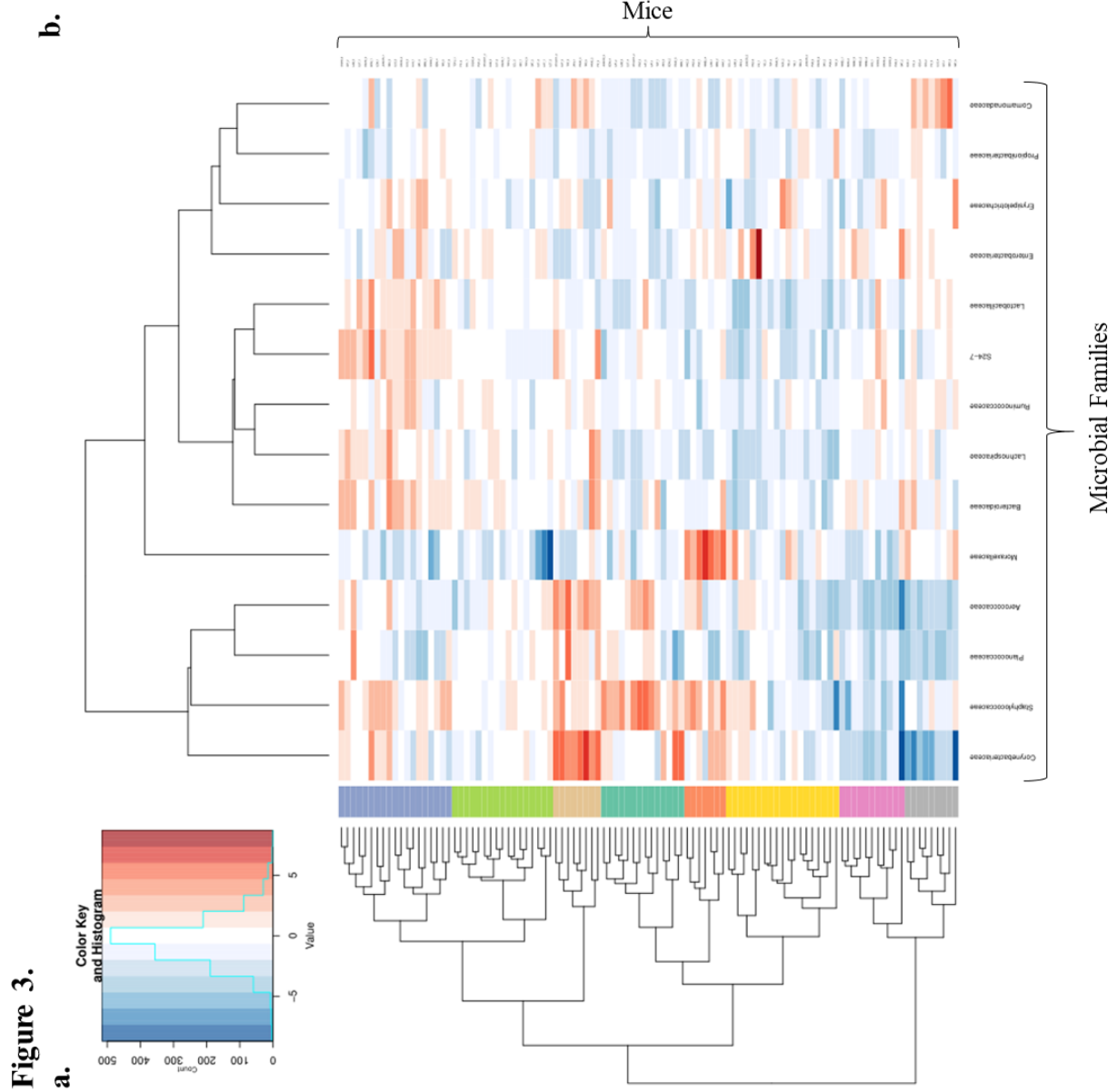
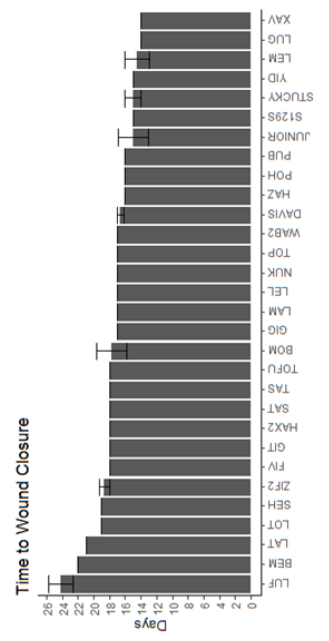
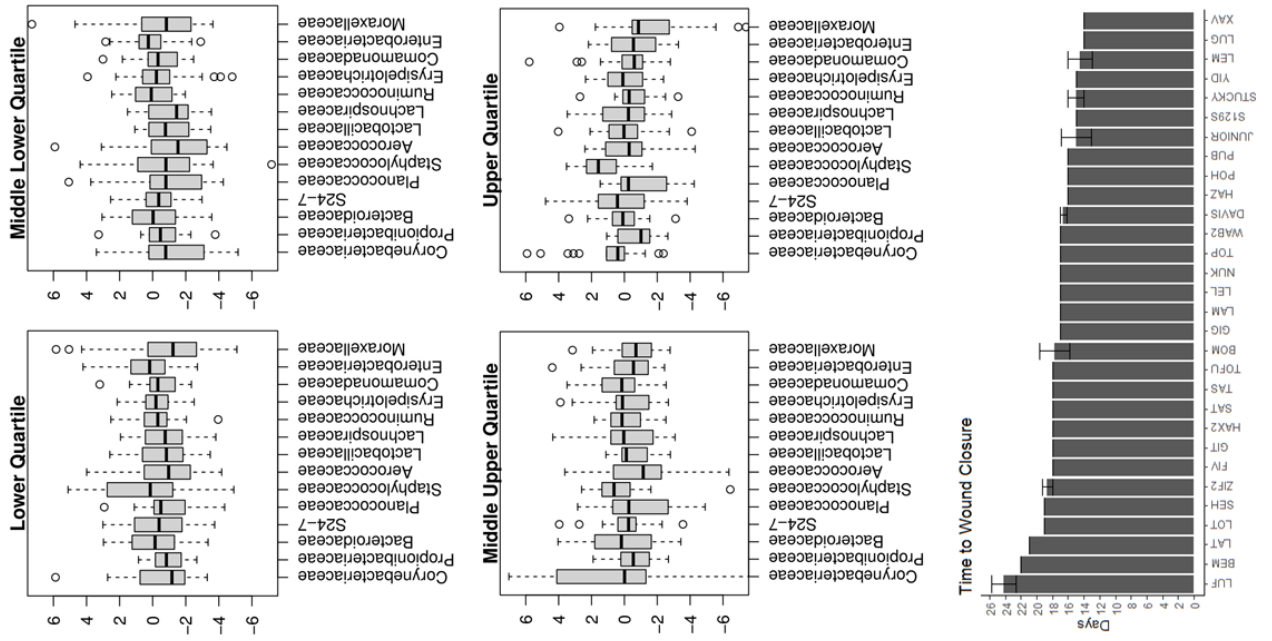


**Figure 3.**

**a.**



348 **Figure 3. Microbiota composition changes from unwounded skin to day 3 post-wounding.**

349 (a) Taking the difference between day 3 post-wounding and unwounded centred-log ratio  
350 matrices shows the relative increase/decrease in microbial abundance during the early stages  
351 of wound healing. No bacterial families show a consistent pattern of increased/decreased  
352 abundance across all mice during wound healing, though many mouse strains show similar  
353 within strain patterns of microbiota changes. (b) Boxplots of bacterial family centred-log ratio  
354 abundance changes during wound healing across all mice, grouped by quartiles of mouse  
355 healing speed (Top and Middle). Each bacterial family shows a large spread of values including  
356 both mice that increase their relative abundance and mice that decrease. No associations can  
357 be seen between a single family of bacteria and faster/slower healing mice. Days to full wound  
358 closure across all mouse strains (Bottom).

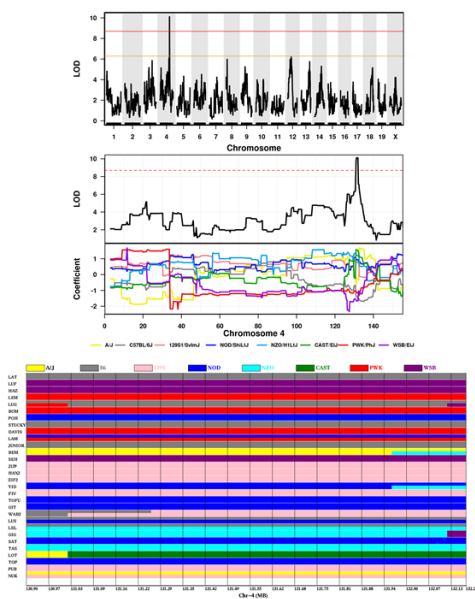
359

360

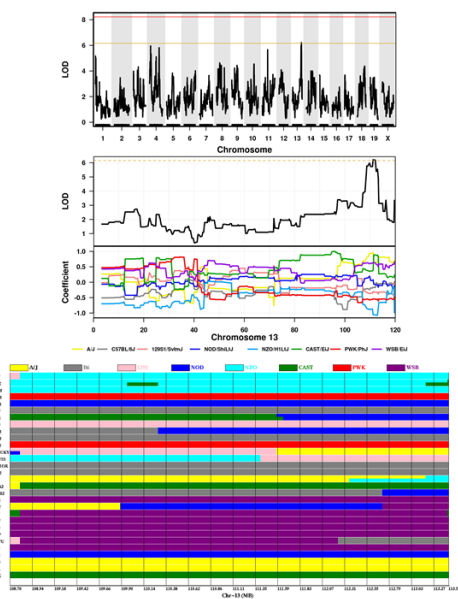
Supplemental 1.

361

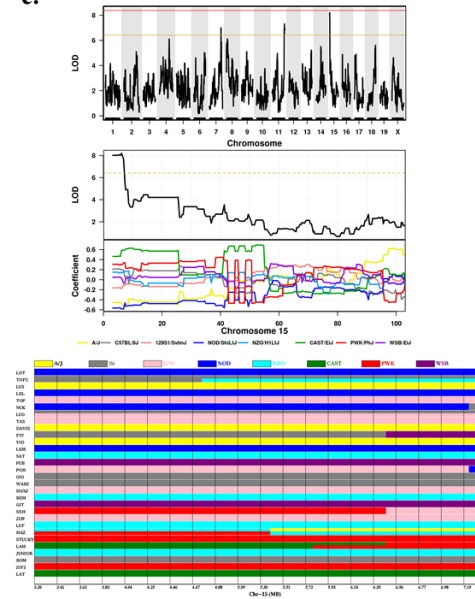
a.



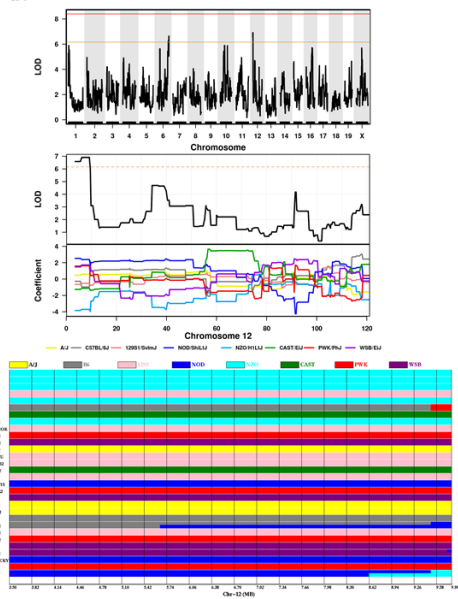
b.



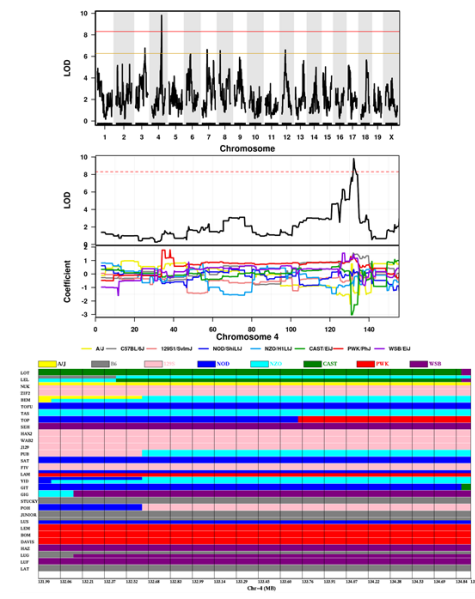
c.



d.



e.

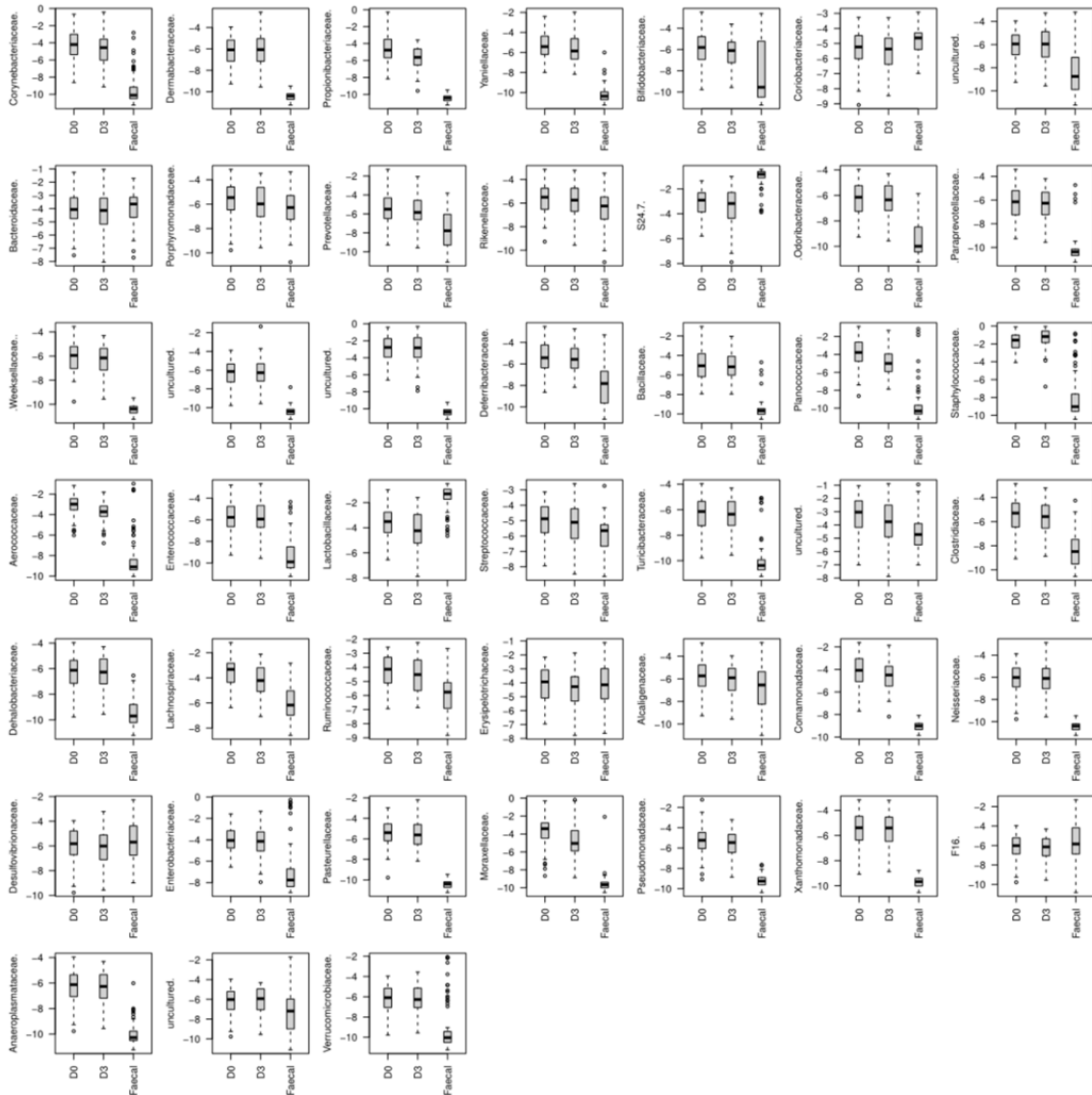


362 **Supplemental 1. GWAS based on haplotype reconstructions of Collaborative Cross**  
363 **mouse genomes. (a)** LOD-score based analysis of *Staphylococcus* centred log-ratio abundance  
364 inputed to GeneMiner. A significant QTL can be identified on chromosome 4, (-2 LOD score  
365 drop region, 130.9-132.2Mbps). Haplotype diagrams indicate the founder strains WSB, CAST  
366 and/or PWK may be responsible for the peak. **(b)** LOD-score based analysis of *Aerococcus*  
367 centred log-ratio abundance inputed to GeneMiner. A suggestive QTL can be identified on  
368 chromosome 13 (-2 LOD score drop region, 108.7-113.51Mbps). Haplotype diagrams indicate  
369 the founder strains NZO, AJ and/or WSB may be responsible for the peak. **(c)** LOD-score based  
370 analysis of Shannon's diversity scores inputed to GeneMiner. A suggestive QTL can be  
371 identified on chromosome 15 (-2 LOD drop region, 3.2-7.4 Mbps). Haplotype diagrams  
372 indicate CAST, AJ and/or NOD as likely responsible for the peak. **(d,e)** PCA-based GWAS  
373 using principal components 1 and 3 **(d, e)**. Suggestive QTL can be found on Chr 12 for both  
374 principle components, though in different regions (-2 LOD drop region PC1, 3.5-9.9Mbps,  
375 PC3, 47.7-60.4Mbps). For principal component 3 **(e)** a significant peak on Chr4 overlapping  
376 the same region as the previous significant peak for *Staphylococcus* can be seen primarily due  
377 to the CAST and PWK founder strains (-2 LOD drop region, 131.9-135Mbps).

378

**Supplemental 2.**

**a.** Log-proportional abundances of all bacterial families (including non-core) (70 mice)



**b.**

Table 1: Mice Used

Strain	Count
BEM	4
BOM	4
DAVIS	5
FIV	5
GIG	3
GIT	2
HAX2	4
HAZ	5
JUNIOR	5
LAM	4
LAT	3
LEL	3
LEM	2
LOT	5
LUF	5
LUG	4
NUK	4
POH	2
PUB	3
S129S	5
SAT	4
SEH	4
STUCKY	3
TAS	3
TOFU	4
TOP	5
WAB2	5
XAV	2
YID	3
ZIF2	4

**c.**

Table 2: Linear Model of Staphylococcus and Aerococcus Diversity Associations

Bacteria	Estimate	P.Value
Staphylococcus	-0.0751578	0.0682618
Aerococcus	-0.1168848	0.0657272

379 **Supplemental 2.** (a) Qualitative summary of all family-level (including non-core skin) log-  
 380 proportional abundances in unwounded, day 3 post-wound, and faecal samples (70 mice).  
 381 *Propionibacteriaceae* and *Bacteroidales* family S24-7 show markedly different abundances  
 382 between skin and faecal samples. (b) List of all Collaborative Cross strains used for initial  
 383 experiment, including mice per strain used (114 total mice). (c) Based on the results from  
 384 differential bacterial genera abundance analysis of most diverse and least diverse mice, we  
 385 modelled Shannon diversity regressed against *Staphylococcus* and *Aerococcus* CLR  
 386 abundances. Negative values for estimate indicate lower diversity values for higher CLR values  
 387 for both *Staphylococcus* and *Aerococcus* with an overall trend across all mice. (d) Schematics  
 388 for the processes of 16S rRNA gene amplicon sequence data analysis.

389

390

391

Haplotype	Genes	Region_(Chr:Mbps)
PWK_PhJ	Laptm5,Matn1	4:130.9-132.2
CAST_EiJ	Epb4.1,Gm10300,Laptm5,Matn1,Mecr,Ptpru,Srsf4,Tmem200b	4:130.9-132.2
WSB_EiJ	Epb4.1,Mecr	4:130.9-132.2
PWK_PhJ	Gpatch3,Rps6ka1	4:131.9-135.0
CAST_EiJ	Aim11,Arid1a,Atpif1,Catsper4,Cnksr1,Epb4.1,Extl1,Eya3,Fam46b, ,Gm10300,Gm7534,Gmeb1,Grrp1,Kdf1,Map3k6,Nr0b2,Nudc,Pdik11, Phactr4,Pigv,Ptafr,Rab42,Rhd,Rpa2,Rsrp1,Sepr1,Smpdl3b, Srsf4,Stx12,Taf12,Tmem200b,Ubxn11,Xkr8,Zdhhc18,Zfp593,Zfp683	4:131.9-135.0
WSB_EiJ	Atpif1,Cd164l2,Epb4.1,Gmeb1,Trnp1	4:131.9-135.0

392

393 **Supplemental 3. Table of candidate genes based on GWAS analysis.** List of genes  
 394 identified in from the QTL on Chromosome 4 present in 2 different GWAS. Genes are taken  
 395 from Sanger Mouse SNP Viewer ([https://www.sanger.ac.uk/sanger/Mouse\\_SnpViewer/rel-1505](https://www.sanger.ac.uk/sanger/Mouse_SnpViewer/rel-1505))  
 396 for the LOD 2 drop region around the QTL peak. A total of 38 genes were identified  
 397 that possessed SNPs specific to any of the haplotypes WSB, PWK or CAST.

398

## 399 **Materials & Methods**

### 400 *Mice*

401 The Collaborative Cross (CC) program used 8 founding strains of mice to produce  
402 several hundred recombinant mouse inbred (RI) strains [20] that were inbred over multiple  
403 generations to greater than 90% homozygosity [43]. This high rate of homozygosity ensures  
404 that most regions of the genome are defined by the genetic contribution from a single founder  
405 strain (haplotype), simplifying analysis. However, the substantial heterogeneity in haplotypes  
406 between different strains can result in marked variation in any phenotype across the CC.  
407 Greatly reduced costs and complexities can be achieved with CC mice, since they are all  
408 genotyped and the founder genome sequences are available at the Sanger Institute  
409 (<https://www.sanger.ac.uk>) [20]. Lastly, the large genetic scope of the CC RI strains, founding  
410 strains were chosen to maximise genetic richness, provides a powerful resource to investigate  
411 murine genetics of complex biological problems.

412 All mice from the CC (114) were housed in the UQ Centre for Clinical Research Animal  
413 Facility. All animal experimentation was conducted in accordance with institutional ethical  
414 requirements and approved by the University of Queensland Animal Ethics Committee. Only  
415 female mice were used with the number of mice per strain varying due to availability. Two  
416 mice from the strains XAV, GIT, LEM and POH were used whereas, all other strains had 3 or  
417 more mice (**Supp.2**).

### 418 *Collection*

419 Mice were anaesthetized with 2% isoflurane and a sterile rayon swab moistened with TE buffer  
420 was used to collect a microbiota sample from a 1.5x1.5cm of dorsal skin, followed by full-  
421 thickness excisional wounds of the same area and second swab was immediately used to sample  
422 this fresh wound (library sizes too small to analyse). This second swab on the excisional wound  
423 served as technical control for contamination for every single mouse. At this initial timepoint  
424 a fresh stool sample was collected. Additional swabs were taken at days 3 and 10 post-  
425 wounding. All samples were stored in 2ml of TE buffer at -80°C for later sequencing.

### 426 *Microbiota community profiling and data analyses*

427 Microbial DNA was extracted from swab samples of dorsal skin using the Maxwell 16 LEV  
428 Buccal Swab DNA kit according to manufacturer's recommendations. The resulting DNA  
429 samples were then used to produce bar-coded PCR amplicon libraries of the V6-V8

430 hypervariable region of the 16S rRNA gene using the universal microbial primers with Illumina  
431 primer overhang adapters as follows:

432 - Forward Primer – 926F:

433 5' - TCG TCG GCA GCG TCA GAT GTG TAT AAG AGA CAG AAA CTY AAA KGA  
434 ATT GRC GG – 3'

435 - Reverse Primer – 1392R:

436 5' - GTC TCG TGG GCT CGG AGA TGT GTA TAA GAG ACA GAC GGG CGG TGW  
437 GTR C – 3'

438 Sequencing used the Illumina MiSeq sequencing platform and protocols developed by  
439 the UQ-Australian Centre for Ecogenomics ([www.ecogenomic.org](http://www.ecogenomic.org)). A sequence Phred quality  
440 threshold of 20 was used and sequences checked for chimeras using USEARCH version  
441 6.1.544 [44]. Mapping and clustering of reads into operational taxonomic units (OTUs) with  
442 97% identity threshold against Greengenes core set database 13.8 [45], was performed using  
443 Quantitative insight into Microbial Ecology (QIIME) version 1.9.1 [46] and PyNast [47]. OTUs  
444 were then compiled into an OUT table for further analysis.

#### 445 *Data Analysis*

446 Shannon measures of alpha diversities were calculated using the ‘Vegan’ package in R [48, 49]  
447 with the function ‘diversity’. The percentage abundance for each bacterial family was  
448 calculated and those bacterial families failing a threshold of 0.1% abundance in 50% or more  
449 mice were removed, leaving a total of 14 ‘core’ bacterial families remaining in the dataset.  
450 Centred log-ratios (CLR) were calculated for all mice using the ‘core’ bacterial families as a  
451 sub-composition. Comparisons of murine skin microbiotas similarities were then performed  
452 using the PERMANOVA and PCA using Aitchison distance (Euclidean distance after CLR  
453 [50]).

#### 454 *QTL Analysis*

455 Significantly differentially abundant genera based on the upper and lower quartiles of diversity  
456 were regressed against mouse genotypes in the GeneMiner software  
457 ([www.sysgen.org/GeneMiner](http://www.sysgen.org/GeneMiner)). GWAS made use of haplotype reconstructions, as detailed  
458 previously [51].



459 We also performed principal component analysis on the centred log-ratios of abundances and  
460 regressed the principal components against mouse genotypes. This style of PCA based GWAS  
461 has been suggested as a way of identifying pleiotropic QTL [24], due to each component  
462 representing a multivariate vector consisting of all phenotypes of interest (in this case all ‘core’  
463 microbiota families).

464

## 465 **Acknowledgements**

466 We would like to thank Geniad Pty Ltd for the generous provision of CC mice. This work was  
467 supported by funding from the National Health and Medical Research Council of Australia  
468 (APP1082438). KK is supported by a Queensland government, Advance Queensland Research  
469 Fellowship.

## 470 **Competing Interests**

471 The authors declare no competing interests.

## 472 **References**

- 473 1. Catinean, A., et al., *Microbiota and Immune-Mediated Skin Diseases-An Overview*.  
474 *Microorganisms*, 2019. **7**(9).
- 475 2. Schoeler, M. and R. Caesar, *Dietary lipids, gut microbiota and lipid metabolism*. *Rev*  
476 *Endocr Metab Disord*, 2019. **20**(4): p. 461-472.
- 477 3. Forsythe, P., et al., *Mood and gut feelings*. *Brain Behav Immun*, 2010. **24**(1): p. 9-16.
- 478 4. Kobyliak, N., O. Virchenko, and T. Falalyeyeva, *Pathophysiological role of host*  
479 *microbiota in the development of obesity*. *Nutr J*, 2016. **15**: p. 43.
- 480 5. Pessi, T., et al., *Interleukin-10 generation in atopic children following oral*  
481 *Lactobacillus rhamnosus GG*. *Clin Exp Allergy*, 2000. **30**(12): p. 1804-8.
- 482 6. Kong, H.H., et al., *Temporal shifts in the skin microbiome associated with disease*  
483 *flares and treatment in children with atopic dermatitis*. *Genome Res*, 2012. **22**(5): p.  
484 850-9.
- 485 7. Min, K.R., et al., *Association between baseline abundance of Peptoniphilus, a Gram-*  
486 *positive anaerobic coccus, and wound healing outcomes of DFUs*. *PLoS One*, 2020.  
487 **15**(1): p. e0227006.
- 488 8. Wolcott, R.D., et al., *Evaluation of the bacterial diversity among and within*  
489 *individual venous leg ulcers using bacterial tag-encoded FLX and titanium amplicon*  
490 *pyrosequencing and metagenomic approaches*. *BMC Microbiol*, 2009. **9**: p. 226.
- 491 9. Grice, E.A., et al., *Topographical and temporal diversity of the human skin*  
492 *microbiome*. *Science*, 2009. **324**(5931): p. 1190-2.
- 493 10. Grice, E.A. and J.A. Segre, *The skin microbiome*. *Nat Rev Microbiol*, 2011. **9**(4): p.  
494 244-53.
- 495 11. McKnite, A.M., et al., *Murine gut microbiota is defined by host genetics and*  
496 *modulates variation of metabolic traits*. *PLoS One*, 2012. **7**(6): p. e39191.



- 497 12. Benson, A.K., et al., *Individuality in gut microbiota composition is a complex*  
498 *polygenic trait shaped by multiple environmental and host genetic factors*. Proc Natl  
499 Acad Sci U S A, 2010. **107**(44): p. 18933-8.
- 500 13. Scharschmidt, T.C., et al., *Matriptase-deficient mice exhibit ichthyotic skin with a*  
501 *selective shift in skin microbiota*. J Invest Dermatol, 2009. **129**(10): p. 2435-42.
- 502 14. Byrd, A.L., et al., *Staphylococcus aureus and Staphylococcus epidermidis strain*  
503 *diversity underlying pediatric atopic dermatitis*. Sci Transl Med, 2017. **9**(397).
- 504 15. Grice, E.A., et al., *A diversity profile of the human skin microbiota*. Genome Res,  
505 2008. **18**(7): p. 1043-50.
- 506 16. Oh, J., et al., *Temporal Stability of the Human Skin Microbiome*. Cell, 2016. **165**(4):  
507 p. 854-66.
- 508 17. Gardiner, M., et al., *A longitudinal study of the diabetic skin and wound microbiome*.  
509 PeerJ, 2017. **5**: p. e3543.
- 510 18. Redel, H., et al., *Quantitation and composition of cutaneous microbiota in diabetic*  
511 *and nondiabetic men*. J Infect Dis, 2013. **207**(7): p. 1105-14.
- 512 19. Loesche, M., et al., *Temporal Stability in Chronic Wound Microbiota Is Associated*  
513 *With Poor Healing*. J Invest Dermatol, 2017. **137**(1): p. 237-244.
- 514 20. Churchill, G.A., et al., *The Collaborative Cross, a community resource for the genetic*  
515 *analysis of complex traits*. Nat Genet, 2004. **36**(11): p. 1133-7.
- 516 21. Ferguson, B., et al., *Melanoma susceptibility as a complex trait: genetic variation*  
517 *controls all stages of tumor progression*. Oncogene, 2015. **34**(22): p. 2879-86.
- 518 22. Murtagh, F., Legendre, P., *Ward's Hierarchical Agglomerative Clustering Method:*  
519 *Which Algorithms Implement Ward's Criterion?* Journal of Classification, 2014. **31**: p.  
520 274-295.
- 521 23. Ward, J.H., *Hierarchical Grouping to Optimize an Objective Function*. Journal of the  
522 American Statistical Association, 1963. **58**: p. 263-244.
- 523 24. Zhang, W., et al., *PCA-Based Multiple-Trait GWAS Analysis: A Powerful Model for*  
524 *Exploring Pleiotropy*. Animals (Basel), 2018. **8**(12).
- 525 25. Shukla, S.D., et al., *Platelet activating factor receptor: gateway for bacterial chronic*  
526 *airway infection in chronic obstructive pulmonary disease and potential therapeutic*  
527 *target*. Expert Rev Respir Med, 2015. **9**(4): p. 473-85.
- 528 26. Iovino, F., et al., *Signalling or binding: the role of the platelet-activating factor*  
529 *receptor in invasive pneumococcal disease*. Cell Microbiol, 2013. **15**(6): p. 870-81.
- 530 27. Stafforini, D.M., et al., *Platelet-activating factor, a pleiotrophic mediator of*  
531 *physiological and pathological processes*. Crit Rev Clin Lab Sci, 2003. **40**(6): p. 643-  
532 72.
- 533 28. Sahu, R.P., et al., *Topical application of a platelet activating factor receptor agonist*  
534 *suppresses phorbol ester-induced acute and chronic inflammation and has cancer*  
535 *chemopreventive activity in mouse skin*. PLoS One, 2014. **9**(11): p. e111608.
- 536 29. Heinz, L.X., et al., *The Lipid-Modifying Enzyme SMPDL3B Negatively Regulates*  
537 *Innate Immunity*. Cell Rep, 2015. **11**(12): p. 1919-28.
- 538 30. Velarde, M.C., et al., *Pleiotropic age-dependent effects of mitochondrial dysfunction*  
539 *on epidermal stem cells*. Proc Natl Acad Sci U S A, 2015. **112**(33): p. 10407-12.
- 540 31. Keyes, B.E., et al., *Impaired Epidermal to Dendritic T Cell Signaling Slows Wound*  
541 *Repair in Aged Skin*. Cell, 2016. **167**(5): p. 1323-1338 e14.
- 542 32. Shettigar, K. and T.S. Murali, *Virulence factors and clonal diversity of*  
543 *Staphylococcus aureus in colonization and wound infection with emphasis on diabetic*  
544 *foot infection*. Eur J Clin Microbiol Infect Dis, 2020. **39**(12): p. 2235-2246.
- 545 33. Kong, H.H., *Skin microbiome: genomics-based insights into the diversity and role of*  
546 *skin microbes*. Trends Mol Med, 2011. **17**(6): p. 320-8.

- 547 34. Yung, D.B.Y., K.J. Sircombe, and D. Pletzer, *Friends or enemies? The complicated*  
548 *relationship between Pseudomonas aeruginosa and Staphylococcus aureus*. Mol  
549 Microbiol, 2021.
- 550 35. Khan, A.A., et al., *Polymorphic Immune Mechanisms Regulate Commensal*  
551 *Repertoire*. Cell Rep, 2019. **29**(3): p. 541-550 e4.
- 552 36. McKenzie, V.J., et al., *Co-habiting amphibian species harbor unique skin bacterial*  
553 *communities in wild populations*. ISME J, 2012. **6**(3): p. 588-96.
- 554 37. Belheouane, M., et al., *Assessing similarities and disparities in the skin microbiota*  
555 *between wild and laboratory populations of house mice*. ISME J, 2020. **14**(10): p.  
556 2367-2380.
- 557 38. Ross, A.A., et al., *Comprehensive skin microbiome analysis reveals the uniqueness of*  
558 *human skin and evidence for phyllosymbiosis within the class Mammalia*. Proc Natl  
559 Acad Sci U S A, 2018. **115**(25): p. E5786-E5795.
- 560 39. Roth, S.A., et al., *The pattern recognition receptor NOD2 mediates Staphylococcus*  
561 *aureus-induced IL-17C expression in keratinocytes*. J Invest Dermatol, 2014. **134**(2):  
562 p. 374-380.
- 563 40. Naik, S., et al., *Commensal-dendritic-cell interaction specifies a unique protective*  
564 *skin immune signature*. Nature, 2015. **520**(7545): p. 104-8.
- 565 41. Srinivas, G., et al., *Genome-wide mapping of gene-microbiota interactions in*  
566 *susceptibility to autoimmune skin blistering*. Nat Commun, 2013. **4**: p. 2462.
- 567 42. Verbanic, S., et al., *Microbial predictors of healing and short-term effect of*  
568 *debridement on the microbiome of chronic wounds*. NPJ Biofilms Microbiomes,  
569 2020. **6**(1): p. 21.
- 570 43. Morgan, A.P. and C.E. Welsh, *Informatics resources for the Collaborative Cross and*  
571 *related mouse populations*. Mamm Genome, 2015. **26**(9-10): p. 521-39.
- 572 44. Edgar, R.C., *Search and clustering orders of magnitude faster than BLAST*.  
573 Bioinformatics, 2010. **26**(19): p. 2460-1.
- 574 45. DeSantis, T.Z., et al., *Greengenes, a chimera-checked 16S rRNA gene database and*  
575 *workbench compatible with ARB*. Appl Environ Microbiol, 2006. **72**(7): p. 5069-72.
- 576 46. Caporaso, J.G., et al., *QIIME allows analysis of high-throughput community*  
577 *sequencing data*. Nat Methods, 2010. **7**(5): p. 335-6.
- 578 47. Caporaso, J.G., et al., *PyNAST: a flexible tool for aligning sequences to a template*  
579 *alignment*. Bioinformatics, 2010. **26**(2): p. 266-7.
- 580 48. Jari Oksanen, F.G.B., Michael Friendly, Roeland Kindt, Pierre Legendre, Dan  
581 McGlenn, Peter R. Minchin, R. B. O'hara, Gavin L. Simpson, Peter Solymos, M.  
582 Henry Stevens, Eduard Szoecs, Helene Wagner, *vegan: Community Ecology Package*.  
583 2019.
- 584 49. Team, R.C., *R: A language and environment for statistical computing*. 2020.
- 585 50. Gloor, G.B., et al., *Microbiome Datasets Are Compositional: And This Is Not*  
586 *Optional*. Front Microbiol, 2017. **8**: p. 2224.
- 587 51. Ram, R. and G. Morahan, *Complex Trait Analyses of the Collaborative Cross: Tools*  
588 *and Databases*. Methods Mol Biol, 2017. **1488**: p. 121-129.

589